Available online at www.sciencedirect.com
ScienceDirect
Journal of Solid State Chemistry 180 (2007) 284–290
JOURNAL OF SOLID STATE CHEMISTRY
www.elsevier.com/locate/jssc

Microemulsion-mediated hydrothermal synthesis and characterization of zircon-type $LaVO_4$ nanowires

Weiliu Fan[a], Xinyu Song[b], Sixiu Sun[a,b,*], Xian Zhao[a,*]

[a]State Key Laboratory of Crystal Materials, Shandong University, People's Republic of China
[b]Department of Chemistry, Shandong University, Jinan 250100, People's Republic of China

Received 19 August 2006; received in revised form 13 September 2006; accepted 9 October 2006
Available online 28 October 2006

Abstract

The zircon-type tetragonal (*t*-) $LaVO_4$ nanowires were controlled synthesized by a new approach, a microemulsion-mediated hydrothermal method, in which the aqueous cores of sodium dodecyl sulfate (SDS)/cyclohexane/*n*-hexanol/water microemulsion were used as constrained microreactors for a controlled growth of *t*-$LaVO_4$ nanocrystals under hydrothermal conditions. The microemulsion exists stably just at room temperature and not under hydrothermal conditions, in addition, the as-obtained nanowires are much larger than the microemulsion droplets, so that the microemulsion does not simply act as a template, but rather directs crystal growth into nanowires presumably by interacting with the surface of the growing crystal. A series of experimental results indicated that several experimental parameters, such as the SDS concentration, the species and content of the cosurfactant play important roles in the morphological control of the *t*-$LaVO_4$ nanocrystals. Possible formation mechanism of *t*-$LaVO_4$ nanowires is also discussed.

Keywords: Microemulsion; Hydrothermal; Zircon-type; $LaVO_4$; Nanowires; Nanorods; Nanotubes

1. Introduction

One-dimensional (1D) inorganic nanomaterials, such as nanowires, nanorods, and nanotubes, have recently attracted much attention because of potential applications in catalysis, optoelectronic devices, and so on [1–4]. Such nanostructures are expected to have unusual characteristics that are amplified through quantum size and shape-specific effects. Reverse micelles or microemulsion systems have been widely used as ideal media to prepare nanoparticles [5–7]. A water-in-oil (w/o) microemulsion is a transparent and isotropic liquid medium with nanosized water pools dispersed in a continuous phase and stabilized by surfactant and cosurfactant molecules at the water/oil interface. These water pools offer ideal microreactors for the formation of nanoparticles. However, some studies, for example, the fabrication of ZnO, $BaCO_3$ nanowires, $BaSO_4$ nanofilaments, CdS, $BaWO_4$ nanorods, and BaF_2 whiskers [8–14] have shown that the microemulsion method can also be used to prepare some 1D nanostructure under certain conditions.

Lanthanide orthovanadates are of interest due to their useful luminescent properties and unusual magnetic characteristics [15–18]. These materials have been employed as highly efficient laser diode pumped micro-lasers, an efficient phosphor and as very attractive polarizer material. Lanthanide orthovanadates crystallize in two polymorphs, namely, monoclinic (*m*-) monazite-type and tetragonal (*t*-) zircon-type. Generally, with increasing ionic radius, Ln^{3+} ions show a strong tendency toward monazite-structured orthovanadate due to its higher oxygen coordination number of 9 as compared with 8 of the zircon one. For this reason $LaVO_4$ chooses monazite type as the thermodynamically stable state while the other orthovanadates normally exist in the zircon type [19,20]. $LaVO_4$ is neither a suitable host for luminescent activators [21,22] nor a promising catalyst [15] due to its ordinary monoclinic (*m*-) monazite structure compared to other orthovanadates. On the contrary, *t*-$LaVO_4$ is expected to possess superior properties, and is expected to be a

*Corresponding authors. Fax: +86 531 88564464.
E-mail addresses: fwl@sdu.edu.cn (W. Fan), ssx@sdu.edu.cn (S. Sun), zhaoxian@icm.sdu.edu.cn (X. Zhao).

0022-4596/$ - see front matter © 2006 Elsevier Inc. All rights reserved.
doi:10.1016/j.jssc.2006.10.019

promising phosphor candidate, as revealed by Yan's research [23]. The main challenge lies in the synthesis of zircon type $LaVO_4$, since it is metastable and cannot be obtained by conventional methods.

In order to obtain *t*-$LaVO_4$, the metastable phased material, solution processes categorized in "soft chemistry" sometimes work well [19,20,24,25]. Yan and co-workers have generated *t*-$LaVO_4$ nanorods with $La(NO_3)_3$ and Na_3VO_4 as starting materials by an ethylenediaminetetraacetic acid mediated hydrothermal method [24]. Recently, our group have demonstrated a facile hydrothermal route for the generation of zircon-type $LnVO_4$ (Ln = La, Nd, Sm, Eu, Dy) nanorods without any templates and/or catalysts [25]. In this method, $LnVO_4$ seeds were formed by reaction of lanthanide nitrate and sodium meta-vanadate in stoichiometric. Nanorods grew over the course of hydrothermal treatment through an Ostwald ripening process by controlling the solution pH. Despite the capability and feasibility of those methods have been successfully illustrated, however, to the best of our knowledge, there have been no reports on zircon type $LaVO_4$ nanowires with aspect ratio larger than 20 to date. Therefore, the development of methods for the synthesis of *t*-$LaVO_4$ nanowires is a major challenge.

In the present work, we report the results of *t*-$LaVO_4$ nanowires with aspect ratio larger than 100 prepared by combining the inverse microemulsion with hydrothermal treatment at 170 °C. Studies found that some related experimental parameters including the concentration of the anionic surfactant, the cosurfactant have great influences on the product morphology. By carefully controlling these experimental parameters, $LaVO_4$ nanostructures with morphologies of nanowires, nanorods, and nanotubes can be efficiently achieved, respectively. The growth mechanism of the 1D nanocrystal has also been discussed in detail.

2. Experimental section

2.1. Chemicals

All the chemicals are of analytical grade and used as received without further purification. Deionized water was used throughout. Lanthanum nitrate, anhydrous sodium meta-vanadate ($NaVO_3$), cationic surfactant sodium dodecyl sulfate (SDS), cyclohexane, and *n*-hexanol were all supplied by the Shanghai Chemical Reagent Company.

2.2. Synthesis method

A quaternary microemulsion, SDS/cyclohexane/*n*-hexanol /water, was selected for the study. As a typical synthesis, two identical solutions were prepared by dissolving SDS (1.81 g) in 20 mL of cyclohexane and 3.5 mL of *n*-hexanol. Next, 1.5 mL of 0.4 M $La(NO_3)_3$ aqueous solution and 1.5 mL of 0.4 M $NaVO_3$ aqueous solution were added to the above solutions, respectively. The mixing solution was stirred for several minutes until it became transparent. After substantial stirring, the two optically transparent microemulsion solutions were mixed. Nucleation occurs immediately after mixing, a turbid yellow emulsion is obtained. The color change indicates $LaVO_4$ nucleus formation, and the particles in this solution were used as seeds for further crystallization to get *t*-$LaVO_4$ nanocrystals. After stirring several minutes, the turbid unstable emulsions can be converted into optically transparent and thermodynamically stable mixtures. Then, NaOH (1 M, 0.9 mL) was added and the microemulsion was aged for another 10 minutes at room temperature. The optically transparent yellowish microemulsion was then transferred to a stainless Teflon-lined autoclave for hydrothermal treatment at 170 °C for 48 h without stirring to make the nanoparticles well crystallized. Naturally cooled to room temperature, the precipitates were separated from the reaction media by centrifugation and were washed with absolute ethanol and distilled water for several times. Finally, the $LaVO_4$ nanosized product was dried under vacuum at 60–70 °C.

Normally, the composition of the four-component microemulsion can be defined by three parameters: ω_0 (the molar ratio between water and SDS), P_0 (the molar ratio between cosurfactant and SDS), and [SDS] (the molar concentration of SDS). In our case, the ω_0 was fixed as 13.3, and the [SDS] and P_0 was varied by modulating the concentration of SDS and cosurfactant, respectively, to control the shape and size of $LaVO_4$ nanoparticles.

2.3. Characterization

The phase purity and crystal structure of the obtained samples were examined by X-ray diffraction (XRD) using a Japan Rigaku D/Max-γA rotation anode X-ray diffractometer equipped with graphite monochromatized Cu Kα radiation ($\lambda = 1.54178$ Å), employing a scanning rate of $0.02^\circ\,s^{-1}$ in the 2θ range from 10° to 75°. The operation voltage and current were maintained at 40 kV and 40 mA, respectively. The morphologies and micro- and nanostructure of the as-synthesized products were characterized by transmission electron microscopy (TEM), carried out using JEOL JEM-100 CXII at an accelerating voltage of 100 kV. Further structural characterization was performed on a Philips Tecnai F30 high-resolution field-emission transmission electron microscope (HRTEM) operating at 300 kV. The samples for these measurements were dispersed in absolute ethanol by being vibrated in the ultrasonic pool. Then the solutions were dropped onto a copper grid coated with amorphous carbon films and dried in air before performance.

3. Results and discussion

The overall crystallinity and purity of the as-synthesized sample were examined by XRD measurements. All of the diffraction peaks in Fig. 1 can be readily indexed to a pure zircon type, i.e. tetragonal phase of $LaVO_4$ [space group:

$I4_1/amd$] with cell constants $a = 7.50$ Å and $c = 6.59$ Å, which are in good agreement with the standard values for the bulk tetragonal $LaVO_4$ (JCPDS 32-0504). No other impurities have been found in the synthesized products.

As a confirmation of XRD analysis, Fig. 2 shows typical TEM images of the t-$LaVO_4$ nanocrystals corresponding to Fig. 1. It was found from Fig. 2a that the products are composed of nanowires with lengths of up to several micrometers, and diameters of about 20 nm, which accounts for their aspect ratios higher than 100. Most of the nanowires are straight and uniform along their axis direction, which is further confirmed from the image (Fig. 2b) obtained with high-resolution transmission electron microscopy (HRTEM). It shows that the as-obtained t-$LaVO_4$ has an obvious anisotropic growth habit, and the nanowire is structurally uniform, free from defects and dislocations. The clearly resolved interplanar spacing of about 0.374 nm correspond to the (200) plane of tetragonal phase $LaVO_4$. Fig. 2c is a corresponding FFT pattern of the HRTEM image (Fig. 2b), which can be indexed to the [010] zone of a tetragonal phase $LaVO_4$. Further studies of the HRTEM image and FFT pattern demonstrate that the direction of t-$LaVO_4$ nanorod growth is along the c-axis, i.e. the [001] direction, which is consistent with the observations from the XRD image.

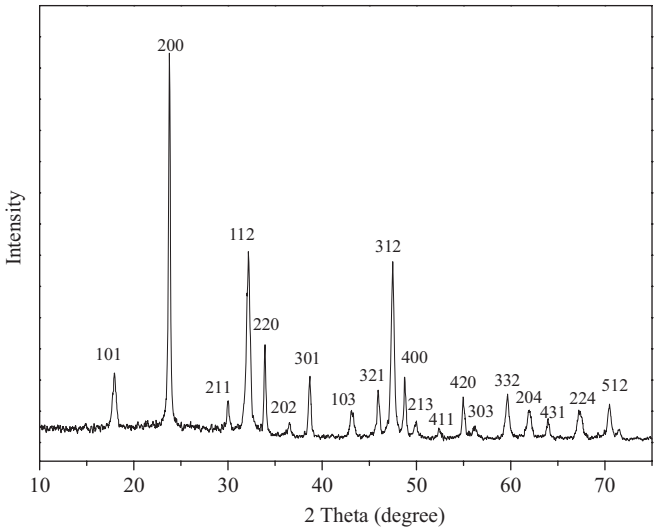

Fig. 1. XRD pattern of the as-prepared t-$LaVO_4$ nanowires under conditions of [SDS] = 0.25 M, $\omega_0 = 13.3$, and $P_0 = 5.78$, via hydrothermal treatment at 170 °C for 48 h.

The evidenced growth of t-$LaVO_4$ nanowires with high aspect ratio suggested that the formation process might involve a directed aggregation growth process mediated by microemulsion droplets, as suggested in previous works [9], in which microemulsion droplets play an important role in modulating crystal size and shape through controlling nucleation rate and nuclei size at the initial stage. Thus, it is much easier to get well-controlled 1D t-$LaVO_4$ nanostructures and it would be possible to tune the crystal shape and diameter by modulating the nucleation rate and nuclei size by altering the molar ratio of quaternary microemulsion components or the chain of the cosurfactant.

Effect of SDS concentration: In the present work, it was found that the concentration of surfactant SDS has great influence on the morphologies of the obtained samples. Fig. 3a presents the nanorods as prepared when [SDS] = 0.18 M, as we can see from the image the rodlike nanoparticles are about 20 nm in diameter with an aspect ratio smaller than 10. Upon increasing the surfactant concentration, the obtained products became longer in length and there was little change in diameter. When the SDS concentration is up to 0.25 M, as can be seen in Fig. 3b, formation of nanowires with aspect ratio more larger than 100 is observed, and the average diameter of the nanowires is about 20 nm. However, a higher surfactant concentration of 0.3 M gave aggregated nanowires and nanorods, it is observed from the TEM image shown in Fig. 3c that besides nanowires, the sample also consists of nanorods. The length and diameter of the nanorods are not uniform, and most of them exceed 50 nm in diameter, with aspect ratio smaller than 10. When increasing the [SDS] to 0.35 M, no t-$LaVO_4$ nanowires can be found; the as-obtained product is composed of conglomerated nanoparticles with diverse morphologies such as short nanorods and irregular shapes which are larger than those observed at 0.18 M (Fig. 3a), as shown in Fig. 3d.

Effect of cosurfactant: Much research focuses on reverse micelles and microemulsion, which indicates that the cosurfactant (alcohol) has important efficacy in controlling the size, shape, and crystallinity of inorganic nanocrystals

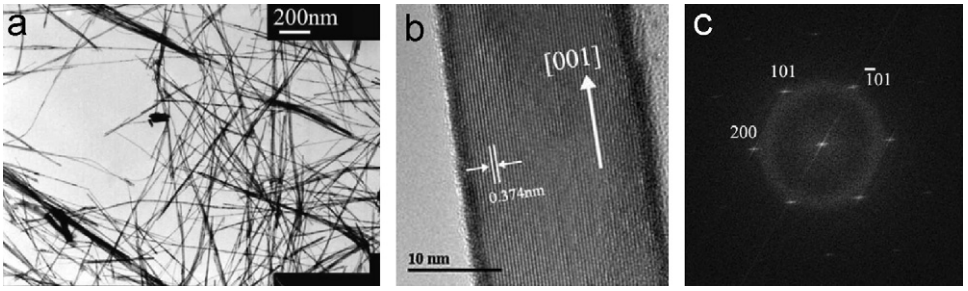

Fig. 2. (a) TEM image of the as-prepared t-$LaVO_4$ nanowires under conditions of [SDS] = 0.25 M, $\omega_0 = 13.3$, and $P_0 = 5.78$, via hydrothermal treatment at 170 °C for 48 h. (b) HRTEM image of a single t-$LaVO_4$ nanowire with a diameter of about 20 nm. (c) Corresponding fast two-dimensional Fourier transform (FFT) pattern of the HRTEM image as shown in (b).

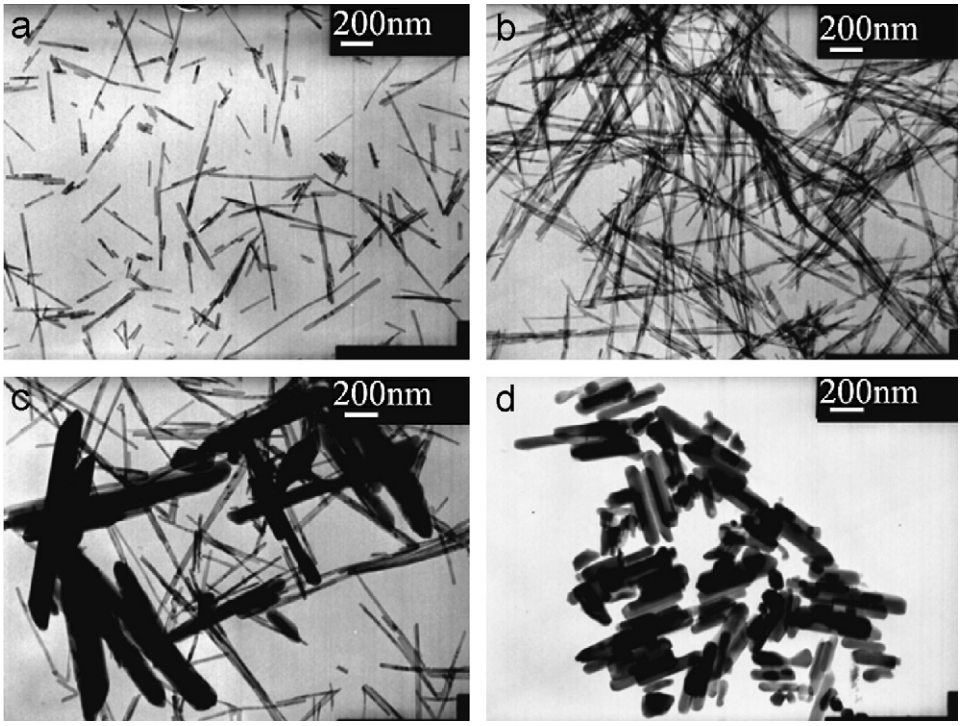

Fig. 3. The TEM images of t-$LaVO_4$ nanocrystals obtained under different surfactant concentration. (a) [SDS] = 0.18 M; (b) [SDS] = 0.25 M; (c) [SDS] = 0.30 M; (d) [SDS] = 0.35 M.

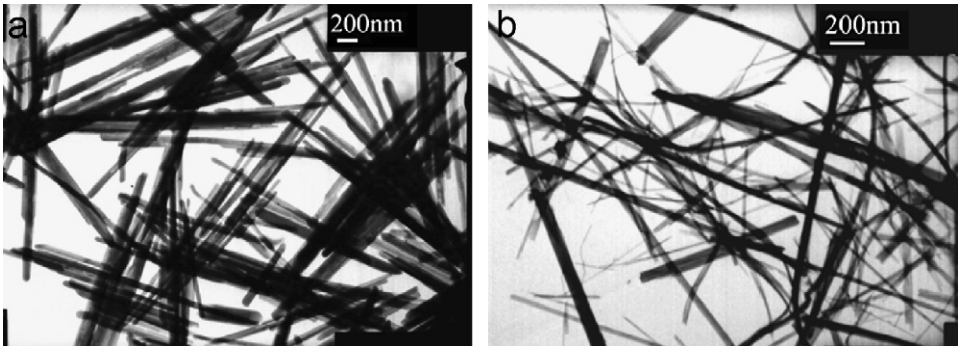

Fig. 4. The TEM images of t-LaVO4 nanocrystals obtained with different species of cosurfactant (a) n-butanol; (b) n-pentanol. Other parameters, such as, [SDS] = 0.25 M, $\omega_0 = 13.3$, and $P_0 = 5.78$, was fixed constant.

[9,26]. In the present work, we found that the length of hydrocarbon chain of cosurfactant is important to modulate the quaternary microemulsion droplets, which afford the possibility to control the nuclei size of $LaVO_4$ formed inside the droplets, and then would affect the diameter of the nanowires during the following formation process.

We replaced n-hexanol by n-butanol or n-pentanol, respectively, to investigate the influence of cosurfactant species on the nanowires. It is indicated that by utilizing n-butanol or n-pentanol instead of n-hexanol, maintaining the other parameters as the sample presented in Fig. 2, the diameter of the obtained t-$LaVO_4$ nanowires increased to about 50–100 nm, as shown in Figs. 4(a) and (b), compared with that of 20 nm when using n-hexanol as cosurfactant. In addition, the as-obtained nanowires aggregated seriously, and the diameters distribution is not uniform. This provides evidence for the modulation effect of the microemulsion on the dimensions of the final products, and we can get that the n-hexanol was more favorable for the formation of t-$LaVO_4$ nanowires with uniform diameters and longer aspect ratio than n-butanol or n-pentanol dose.

The role played by the cosurfactant can be summarized in two different actions [26]. On one hand, the increased flexibility of the water-in-oil interface is generally considered responsible for increasing the exchange rates of micelles, thus allowing exchange of solubilized matter and, consequently, Ostwald ripening. On the other hand, the absorption on the nanocrystal surface determines the

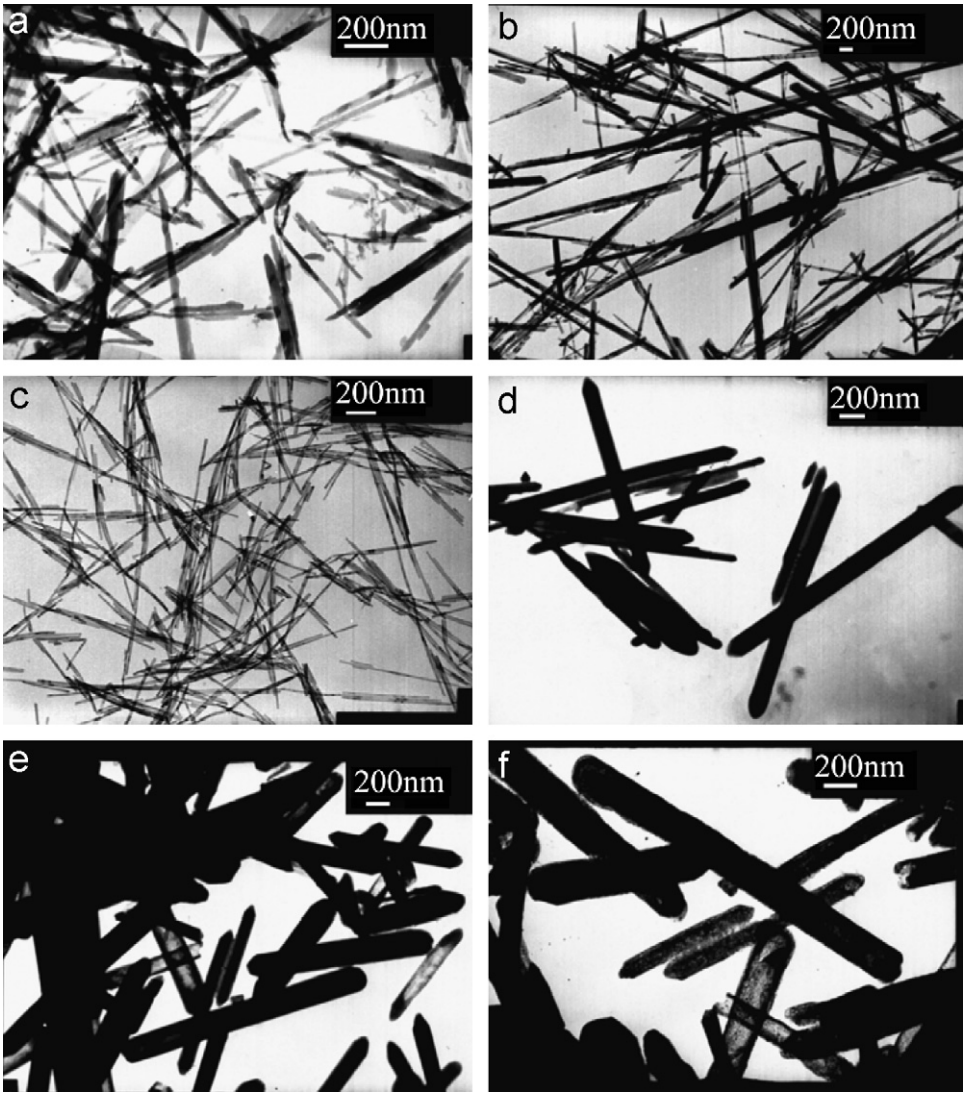

Fig. 5. The TEM images of t-$LaVO_4$ 1D nanostructures obtained under different n-hexanol content. (a) $P_0 = 3.85$; (b) $P_0 = 5.13$; (c) $P_0 = 5.78$; (d) $P_0 = 7.06$; (e) and (f) $P_0 = 8.35$. Other parameters, such as, [SDS] = 0.25 M, and $\omega_0 = 13.3$ was fixed constant.

particle's stabilization in solution, acting as a capping agent, and leading to controlling the morphology of the final nanocrystals.

As far as the quaternary SDS microemulsion is concerned, it is found that interface rigidity can be easily adjusted by changing the parameter of P_0, i.e. the molar ratio between cosurfactant (n-hexanol) and SDS. By varying the P_0 from 3.85 to 8.35 while maintaining other parameters, the shape and size of the products changed obviously, as shown in the representative TEM images in Fig. 5. With lower n-hexanol concentration ($P_0 = 3.85$), mainly short bone-like nanorods precipitated (Fig. 5a). These nanorods are not uniform in diameter and not so smooth. By increasing n-hexanol content to $P_0 = 5.13$, longer nanowires are obtained and the aspect ratio reaches about 70, but the obtained nanowires are inclined to aggregated together (Fig. 5b). In our experimental work, the choice of $P_0 = 5.78$ was proved to produce predominantly uniform nanorods about 20 nm in diameter and with lengths up to several micrometers, as shown in Fig. 5c. With further increasing the n-hexanol content to $P_0 = 7.06$, the anisotropic growth of t-$LaVO_4$ nanocrystals along c-axis is restrained, no nanowires with aspect ratio larger than 100 can be found, as can be seen from Fig. 5d, the rodlike shape of as-prepared samples is relatively uniform with an average diameter around 150 nm and aspect ratio about 15. From the TEM image (Fig. 5d) we can also find that the ends of the rods evolve from prism- to pyramid-like shapes, this is also ascribed to the crystal anisotropic growth habit of t-$LaVO_4$ nanocrystals in the given reaction circumstance. In the system described above, when the n-hexanol content was increased to $P_0 = 8.35$, it was interesting to find tube-like t-$LaVO_4$ nanocrystals were formed. Figs. 5e and 5f show the typical TEM images of the as-prepared nanotube, from which we can see that the nanotubes are 100–200 nm in diameter and several

micrometers in length, the thickness of the tube skin is only tens of nanometers. This also provides evidence for the modulation effect of the microemulsion on the morphology of the final products.

Proposed mechanism: The mechanism of nucleation and growth of 1D nanostructure is a complex process of simultaneous chemical reactions and self-assembly. Normally, without the assistance of additive, the crystallization of t-$LaVO_4$ with $La(NO_3)_3$ and $NaVO_3$ as source materials also shows a tendency toward 1D nanostructures under hydrothermal conditions by tuning the pH value of the growth solution, but can only result in nanorods shape with low aspect ratio ($\leqslant 10$), as can be referred in our former report [25]. In that case, we think Ostwald ripening is the dominant mechanism of the nanorods growth: the formation of tiny crystalline nuclei in a supersaturated medium occurred at first, and this was followed by crystal growth. The larger particles grew at the cost of the small particles; reduction in surface energy is the primary driving force for crystal growth and morphology evolution, due to the difference in solubility between the larger particles and the small particles, according to the well-known Gibbs–Thomson law. As the reaction continued, the irregular nanoparticles vanished and longer nanorods formed.

But in the present work, when the microemulsion-based system is utilized, the formation of homogeneous t-$LaVO_4$ nanowires might be induced and achieved, so for the growth mechanism of t-$LaVO_4$ nanowires with high aspect ratio, the roles of microemulsion should be taken into account.

Initially, the microemulsion acts as a confined space, effectively inhibiting $LaVO_4$ nucleus growth in the early stages of synthesis as compared to bulk syntheses. The precursor, $LaVO_4$ nucleus formed at room temperature after mixing the reactants, can be dispersed homogeneously inside the droplets of the microemulsion. With this aspect, the microemulsion droplets can act as microreactors, and play a role in controlling nucleation rate and nuclei size during this stage, which would eventually affect the shape formation of the final products. When temperature rises with hydrothermal treatment to improve the crystallinity, the reverse micelles in microemulsion may be broken, resulting in nucleus aggregation and growth, in this process it appears that the other aspect of the microemulsion, namely, surfactant/cosurfactant adsorption at the vanadate surface, becomes important for controlling the morphology of the final products. The presence of these various species of microemulsion during the nanocrystal growth modifies the growth of certain crystal faces. Most of the changes are based on the existence of a more or less epitaxial adsorption layer on the crystal. This layer is composed of surfactant (SDS) or cosurfactant (*n*-hexanol) whose precise roles are as yet uncertain, which provided a favorable environment for the crystallization into a single-crystalline 1D nanostructure along a preferred orientation. From this it can be concluded that the SDS microemulsion is the key parameter in the controlled-synthesis of t-$LaVO_4$ nanowires.

The experiments showing how morphology is influenced by the surfactant content support the hypothesis that it is the surfactants that affect the morphology evolution of the final products. Also, the results indicate that the nature of the water-in-oil interface interface of the SDS microemulsion, which can be tuned by changing the species and content of the cosurfactant, also strongly influences the shape and size of the obtained nanocrystals. But unfortunately the detailed growth mechanism of the t-$LaVO_4$ nanotubes is yet uncertain and is in progress.

4. Conclusion

In summary, we have developed a microemulsion-mediated hydrothermal method to prepare zircon type t-$LaVO_4$ nanowires. The quaternary SDS microemulsion is responsible for the control the morphology of the products. By tuning the composition of microemulsions, t-$LaVO_4$ nanorods with aspect ratio smaller than 20 and t-$LaVO_4$ nanotubes can also be controlled synthesized. The diversity of the observed crystal morphology suggests that there is a complex interplay of reagent confinement, crystal growth rate, and adsorption of some of the microemulsion components onto the growing crystal surface in affecting crystal nucleation and growth. On the basis of the results presented, a mechanism is proposed illustrating the role of both the confined space presented by the microemulsion as well as the importance of the surfactant–vanadate interactions leading to the formation of the t-$LaVO_4$ 1D nanostructures.

References

[1] J. Hu, T.W. Odom, C.M. Liber, Acc. Chem. Res. 32 (1999) 435.
[2] Z.L. Wang, Adv. Mater. 12 (2000) 1295.
[3] J. Holms, K.P. Johnston, R.C. Doty, B.A. Korgel, Science 287 (2000) 1471.
[4] (a) Y.N. Xia, P.D. Yang, Y.G. Sun, Y.Y. Wu, B. Mayers, B. Gates, Y.D. Yin, F. Kim, H.Q. Yan, Adv. Mater. 15 (2003) 353;
(b) I. Lisiecki, A. Filankembo, H. Sack-Kongehl, K. Weiss, M.P. Pileni, J. Urban, Phys. Rev. B 61 (2000) 4968;
(c) N. Pinna, M. Willinger, K. Weiss, J. Urban, R. Schlögl, Nano. Lett. 3 (2003) 1131;
(d) N. Pinna, U. Wild, J. Urban, R. Schlögl, Adv. Mater. 15 (2003) 329.
[5] (a) M. Schwuger, K. Stickdom, R. Schomacker, Chem. Rev. 95 (1995) 849;
(b) M.P. Pileni, J. Phys. Chem. 97 (1993) 6961;
(c) M.P. Pileni, Langmuir 13 (1997) 3266.
[6] L.M. Gan, B. Liu, C.H. Chew, S.J. Xu, S.J. Chua, G.L. Loy, G.Q. Xu, Langmuir 13 (1997) 6427.
[7] P. Feng, X. Bu, G.D. Stucky, D.J. Pine, J. Am. Chem. Soc. 122 (2000) 994.
[8] J. Zhang, L.D. Sun, H.Y. Pan, C.S. Liao, C.H. Yan, New J. Chem. 26 (2002) 33.
[9] J. Zhang, L.D. Sun, X.C. Jiang, C.S. Liao, C.H. Yan, Cryst. Growth Des. 4 (2004) 309.
[10] L.M. Qi, J.M. Ma, H.M. Cheng, Z.G. Zhao, J. Phys. Chem. B 101 (1997) 3460.

[11] J.D. Hopwood, S. Mann, Chem. Mater. 9 (1997) 1819.
[12] P. Zhang, L. Gao, Langmuir 19 (2003) 208.
[13] S. Kwan, F. Kim, J. Akana, P.D. Yang, Chem. Commun. (2001) 447.
[14] M.H. Cao, C.W. Hu, E.B. Wang, J. Am. Chem. Soc. 125 (2003) 11196.
[15] Z.M. Fang, Q. Hong, Z.H. Zhou, S.J. Dai, W.Z. Weng, H.L. Wan, Catal. Lett. 61 (1999) 39.
[16] M. Ross, IEEE J. Quantum Electron. 11 (1975) 938.
[17] (a) J.R. O'Connor, Appl. Phys. Lett. 9 (1966) 407;
(b) A.K. Levine, F.C. Palilla, Appl. Phys. Lett. 5 (1964) 118;
(c) B.C. Chakoumakos, M.M. Abraham, L.A. Boatner, J. Solid State Chem. 109 (1994) 197.
[18] (a) Y. Oka, T. Yao, N. Yamamoto, J. Solid State Chem. 152 (2000) 486;
(b) L.D. Sun, Y.X. Zhang, J. Zhang, C.H. Yan, C.S. Liao, Y.Q. Lu, Solid State Commun. 124 (2002) 35.
[19] F.C. Palilla, A.K. Levine, M.J. Rinkevics, J. Electrochem. Soc. 112 (1965) 776.
[20] U. Rambabu, D.P. Amalnerkar, B.B. Kale, S. Buddhudu, Mater. Res. Bull. 35 (2000) 929.
[21] R.C. Ropp, B. Carroll, J. Inorg. Nucl. Chem. 35 (1973) 1153.
[22] M.E. Escobar, E.J.Z. Baran, Anorg. Allg. Chem. 114 (1978) 273.
[23] C.J. Jia, L.D. Sun, F. Luo, X.C. Jiang, L.H. Wei, C.H. Yan, Appl. Phys. Lett. 84 (2004) 5305.
[24] C.J. Jia, L.D. Sun, L.P. You, X.C. Jiang, F. Luo, Y.C. Pang, C.H. Yan, J. Phys. Chem. B 109 (2005) 3284.
[25] W.L. Fan, W. Zhao, L.P. You, X.Y. Song, W.M. Zhang, H.Y. Yu, S.X. Sun, J. Solid State Chem. 177 (2004) 4399.
[26] M.L. Curri, A. Agostiano, L. Manna, M.D. Monica, M. Catalano, L. Chiavarone, V. Spagnolo, M. Lugara, J. Phys. Chem. B 104 (2000) 8391.